

# Hot Bottom Burning in the envelope of SAGB stars

P. Ventura<sup>1\*</sup> and F. D’Antona<sup>1</sup>

<sup>1</sup>*INAF-Osservatorio Astronomico di Roma, Via Frascati 33, Monte Porzio Catone 00040, Italy*

Accepted . Received ; in original form

## ABSTRACT

We investigate the physical and chemical evolution of population II stars with initial masses in the range 6.5–8  $M_{\odot}$ , which undergo an off centre carbon ignition under partially degenerate conditions, followed by a series of thermal pulses, and supported energetically by a CNO burning shell, above a O-Ne degenerate core. In agreement with the results by other research groups, we find that the O-Ne core is formed via the formation of a convective flame that proceeds to the centre of the star. The evolution which follows is strongly determined by the description of the mass loss mechanism. Use of the traditional formalism with the super-wind phase favours a long evolution with many thermal pulses, and the achievement of an advanced nucleosynthesis, due the large temperatures reached by the bottom of the external mantle. Use of a mass loss recipe with a strong dependence on the luminosity favours an early consumption of the stellar envelope, so that the extent of the nucleosynthesis, and thus the chemical composition of the ejecta, is less extreme. The implications for the multiple populations in globular clusters are discussed. If the “extreme” populations present in the most massive clusters are a result of direct formation from the super-AGB ejecta, their abundances may constitute a powerful way of calibrating the mass loss rate of this phase. This calibration will also provide informations on the fraction of super-AGBs exploding as single e-capture supernova, leaving a neutron star remnant in the cluster.

**Key words:** Stars: abundances – Stars: AGB and post-AGB

## 1 INTRODUCTION

The deep spectroscopic surveys of Globular Clusters (GC) stars performed in the last decades have revealed star-to-star differences, that trace well defined abundance patterns, involving all the “light” elements, up to Aluminium (Norris et al. 1981). The discovery that stars belonging to the main sequence or the sub-giant branch show the same patterns of abundances present in the red giants of the same cluster (Carretta 2006), indicated that some self-enrichment mechanism has been active in GCs, and that a new, second, stellar generation (SG) formed, from the ashes of the evolution of older objects, belonging to a first generation (FG). A key-point towards the understanding of the processes behind these observational results is the large fraction of stars with the anomalous chemistry, that hardly drops below 50% of the total number of stars examined, and exceeds 80% in some clusters (Carretta et al. 2009a,b). The Oxygen-Sodium anticorrelation is by far the most studied, and has been confirmed to exist in practically all the GCs investigated, although the slope of the O-Na relationship, and the lowest oxygen abundances detected, vary considerably

from cluster to cluster. In many clusters a Mg-Al anticorrelation is also detected, although the extent of the magnesium depletion is still debated (Cohen & Melendez 2005). Unlike the O-Na trend, the Mg-Al relationship is not of straight interpretation, because not only the slope (if any), but also the maximum magnesium and the minimum aluminium mass fractions, which are commonly interpreted as the abundances of the primordial population, change from cluster to cluster (Carretta et al. 2009b). Photometric signatures are generally less striking than the spectroscopic evidence, apart from the presence of very anomalous “blue” main sequences (bMS) in two among the most massive clusters ( $\omega$  Cen and NGC 2808 Bedin et al. 2004; Piotto et al. 2005; D’Antona et al. 2005; Piotto et al. 2007) and by the presence of very extended horizontal branches and very luminous RR Lyrae in two metal rich clusters –NGC 6388 and NGC 6441. Both these features indicate the presence of a very helium rich population ( $Y \gtrsim 0.36$ – $0.38$ ) in these four clusters (e.g. Norris 2004; Caloi & D’Antona 2007).

Three distinct scenarios have been proposed so far for the progenitors of the SG, each of which must face some difficulties in reconciling the theoretical predictions with the observational evidence: a) winds from massive AGBs (Ventura et al. 2001), b) ejecta from fastly rotating massive stars (Decressin et al. 2007), and c) massive binaries

\* E-mail: ventura@oa-roma.inaf.it (AVR)

(de Mink et al. 2009). All these polluters together, plus the possible contribution of stellar collisions, have been proposed by Sills & Glebbeek (2010). In this work we focus on the first hypothesis, already outlined on qualitative grounds by Ventura & D'Antona (2008) and Ventura & D'Antona (2009), and fixed on a most robust framework by two seminal papers, computing first the possible hydrodynamical and N-body evolution, and further exploring the chemical evolution of protoclusters (D'Ercole et al. 2008, 2010). In these latter works, it is suggested that the SG forms in a cooling flow established in the GC core by the gas ejected at low velocity by massive AGBs. This process is restricted to a narrow time interval  $\lesssim 10^8$ yr, thus allowing only the contribution of stars with masses  $M \geq 5M_{\odot}$ , after which star formations stops, due to the onset of SNIa explosions. The loss of stars from the outskirts of the cluster helps diminishing the FG/SG stars number ratio, because this mechanism hardly involves, in a first phase, the core born SG objects.

D'Ercole et al. (2008), following Pumo et al. (2008), also suggested that in the most massive clusters a preminent role in the star forming process is played by super-AGB (SAGB) stars, defined as objects with initial masses in the range  $(9-11M_{\odot})^1$  that undergo off-center carbon ignition in partially degenerate conditions, and end-up their evolution as O-Ne white dwarfs. They showed, by means of hydrodynamical simulations, that stars belonging to the very high helium populations quoted above, found only in the most massive clusters, are possibly formed *directly* from the winds of the SAGBs, before mixing with pristine gas favours a less extreme chemistry. SAGBs, according to Siess (2007), have helium envelope abundance  $Y=0.36 - 0.38$  after the second dredge up, and as such are the only viable candidate for the bMSs. Unlike helium, the other yields of SAGBs are the result of mass loss and hot bottom burning (HBB) in the phase of thermal pulses following the formation of the O-Ne core. Common interpretation attributes to them the most extreme chemical anomalies found in the clusters having the bMS (see, e.g. D'Ercole et al. 2010), but a full confirmation will have to wait for accurate abundance determinations of stars belonging to the bMSs. It is well known that the massive AGB yields are dramatically dependent of several uncertain input physics parameters, such as convection model, mixing and nuclear cross sections (Ventura & D'Antona 2005a,b), and we can expect similar, or even more extreme, uncertainties in the SAGB mass range.

Theoretical models of SAGBs have been first presented in a series of paper by Garcia-Berro & Iben (1994), Iben et al. (1997), Ritossa et al. (1996), Ritossa et al. (1999), until the recent updates by Siess (2006) and Siess (2007): the carbon burning phase in these models is described in terms of a burning flame, that propogates inwards, until carbon burning reaches the center. The main effects due to overshooting (Gil-Pons et al. 2007), and thermohaline mixing (Siess 2009) were also investigated and discussed. The recent work by Siess (2010) presents the first

<sup>1</sup> The range of masses involved depends on the assumptions regarding the overshooting from the convective core during the two main phases of nuclear burning: overshooting increases the size of the convective core, and thus shifts the masses involved to lower values.

database of yields of SAGBs with different mass and metallicity, and include also the Thermal Pulses (TP) phase that follows the extinction of carbon burning. Finally, the investigation by Doherty et al. (2010) outlined the robustness of the theoretical description of these evolutionary phases, showing that when a sufficiently accurate temporal resolution is adopted, results obtained with different codes show a satisfactory agreement.

Siess (2010) SAGB computations are based on physical assumptions very different from our own (Ventura & D'Antona 2009), that we have already applied to the interpretation of GC abundance patterns. Here we extend our models to the range of SAGB masses, to show how the results depend on detailed physical inputs and, mostly, on the assumed mass loss law. In fact, on the chemical side, we expect uncertainties on the yields' computation, because the mass loss description, the efficiency of the convective modelling, the choice of the nuclear cross-sections, are all expected to play a role in the physical, and thus chemical description of the evolutionary phases following the formation of the O-Ne core. The fate of these stars is also highly uncertain, as it depends on the velocity with which the convective mantle is consumed, and, in more details, whether this process is completed before electron captures begin inside the core (e.g. Poelarendes et al. 2008).

Our aim is thus to explore the uncertainties associated to the yields of these stars, and particularly to the oxygen and sodium mass fractions, because mostly these two elements are investigated in the spectroscopic surveys of GC stars. We will also consider the helium content in the ejecta, and the magnesium and aluminum yields, following the scheme given in Ventura & D'Antona (2009) (but see also D'Ercole et al. 2010).

## 2 HOT BOTTOM BURNING: THE DIFFERENT FATE OF OXYGEN, SODIUM MAGNESIUM AND ALUMINIUM

Massive AGBs do not obey to the classic luminosity vs. core mass relationship found by Paczynski (1970), because this latter is based on the assumption that a radiative buffer is present between the H-burning shell and the bottom of the convective envelope, whereas in massive AGBs the bottom of the convective envelope eventually overlaps with the H-burning shell, so that part of the nuclear energy is generated directly into the external mantle (Blöcker & Schönberner 1991). This phenomenon, normally indicated as Hot Bottom Burning, is of paramount importance for the topic of the self-enrichment by massive AGBs, because it is an efficient way of polluting the stellar environment with matter that was nuclearly processed in repeated proton-capture reactions (Cottrell & Da Costa 1981; Ventura et al. 2001).

In a series of papers, Ventura & D'Antona (2005a, 2008, 2009) showed that HBB is expected to operate efficiently in all popII AGB models with initial masses  $M \gtrsim 4M_{\odot}$ , provided that a high efficiency convection model is adopted, e.g. the Full Spectrum of Turbulence description for turbulent convection (Canuto & Mazzitelli 1991). The surface chemistry is consequently modified.

Oxygen is burnt by proton capture; the rate of destruction increases for higher temperatures, and is thus stronger

in the more massive models, whose core mass is larger. In the most massive AGBs, i.e. the highest masses not undergoing carbon ignition ( $\sim 6 - 6.3M_{\odot}$  in Ventura & D'Antona 2008), the final oxygen abundance is a factor of  $\sim 20$  smaller than the initial mass fraction (see Figure 2 in Ventura & D'Antona 2008), and the average oxygen in the ejecta is decreased by a factor  $\sim 7$ . When  $M$  increases, the trend with mass tends to flatten, and eventually is reversed (see Table 2 in Ventura & D'Antona 2009), because the higher temperatures, that tend to decrease the oxygen content of the ejecta, are partly compensated by the larger mass loss, suffered by the most massive models in the early AGB phases, when the surface oxygen was still rather large. This is an effect of the steep increase of mass loss with luminosity of the Blöcker (1995) recipe.

The behaviour of sodium is more complex, as it is a result of a production channel and two destruction reactions, with very different sensitivity to the temperature in the range of interest here (Hale et al. 2002, 2004). For  $T < 60\text{MK}$  the reaction of proton capture by  $^{22}\text{Ne}$  nuclei dominates, thus producing great amounts of sodium; at higher temperatures, the destruction channels via proton capture take over, and sodium is destroyed, reaching an equilibrium value, at which creation and burning rates cancel each other (see Fig.4 in Ventura & D'Antona (2008)). Two consequences arise from the above description:

- Unlike oxygen, the predictions concerning the sodium yields are not robust, given the uncertainties of the p-capture reactions of the Ne-Na cycle.
- The temperature sensitivity of the  $^{23}\text{Na}+\text{p}$  reaction, much steeper compared to the production channel, if confirmed, is necessarily associated to a direct correlation between the average oxygen and sodium content of the ejecta (Denissenkov & Herwig 2003; Herwig 2004; Karakas & Lattanzio 2007; Ventura & D'Antona 2008); only in the very early AGB phases, when oxygen burning is active and the sodium production prevails over destruction, oxygen and sodium show an opposite behaviour.

HBB modifies the surface abundances of magnesium and aluminium too.  $^{24}\text{Mg}$  is destroyed when  $T_{bce} \sim 60 - 70\text{MK}$ , and  $^{27}\text{Al}$  is produced by a proton-capture chain, that also increases the surface mass fractions of the two heavy magnesium isotopes,  $^{25}\text{Mg}$  and  $^{26}\text{Mg}$ . Ventura & D'Antona (2008) find that the extent of the Al production (hence, of the depletion of magnesium) increases with mass in massive AGBs, though an upper limit of  $[\text{Al}/\text{Fe}] \sim 1$  is reached, which is again due to the high mass loss experienced by the most massive stars at the beginning of the AGB phase. These results were obtained by adopting the upper limits for the two proton capture reactions by the heavy magnesium isotopes, although the recent analysis by D'Ercole et al. (2010) on M4 recommends the use of the standard cross sections. The uncertainties associated to the relevant cross-sections of the Mg-Al chain render the results uncertain by  $\sim 0.3$  dex (Ventura & D'Antona (2008), but see also the discussion in Izzard et al. (2007)).

### 3 THE MODELS

#### 3.1 Physical and chemical inputs

To investigate the nucleosynthesis at the bottom of the external mantle of SAGB stars after the carbon burning phase, we calculate models with the standard chemistry typical of intermediate metallicity GCs, i.e.  $Z=0.001$ ,  $Y=0.24$ , and an  $\alpha$ -enhanced mixture, with  $[\alpha/\text{Fe}]=+0.4$  (Grevesse & Sauval 1998).

The nuclear network includes the most important reactions involving all the chemical species up to silicon. Most of the cross-sections were taken from the NACRE compilation (Angulo et al. 1999); to maintain consistency with Ventura & D'Antona (2005a,b, 2008) we used the upper limits for the proton capture reactions by  $^{25}\text{Mg}$  and  $^{26}\text{Mg}$ . This choice maximizes the aluminum production; a full description of the Mg-Al production and destruction will be given in a forthcoming paper. The reaction rates of the  $^{14}\text{N}(p,\gamma)^{15}\text{O}$  reaction were taken from Formicola et al. (2004), whereas the cross sections by Hale et al. (2002) and Hale et al. (2004) were adopted for the reactions of the Ne-Na cycle. Sodium production was maximized by adopting the upper limit for the proton capture reaction by  $^{22}\text{Ne}$  nuclei.

Mass loss was modelled according to Blöcker (1995), while some comparison sequences follow the recipe by Vassiliadis & Wood (1993). Nuclear burning and convective mixing were coupled by means of a diffusive approach (Cloutman & Eoll 1976). Convective eddies are allowed to overshoot into regions of radiative stability during both hydrogen and helium nuclear burning in the core; this extra-mixing is simulated by an exponential decay of velocities beyond the formal border fixed via the classic Schwarzschild criterium, with an e-folding distance  $\zeta H_p$ , with  $\zeta = 0.02$ , in agreement with a calibration based on the observed widths of the main sequences of open clusters, presented in Ventura et al. (1998). The range of masses investigated is 6.5-8 solar masses; this range is to be compared with the interval 8-9 $M_{\odot}$  found for the same chemistry by Siess (2010). The different assumptions on overshooting are the cause of the difference in the mass range of SAGBs. The involved core masses in fact are very similar in the two investigations (see Figure 2). The results are also in agreement with the exploration on the effects of overshooting by Gil-Pons et al. (2007).

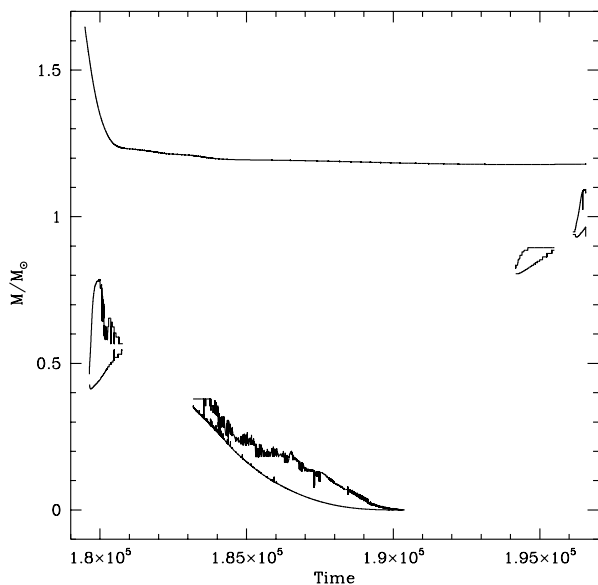
#### 3.2 The Carbon burning phase

The main physical properties concerning the C-burning phase are presented in Tab. 1, where for the various masses involved we show the time elapsed from the end of the core-He burning phase to the ignition of the first C-burning episode, the mass of the CO core when carbon burning starts, the mass of the layer at which carbon is ignited, the maximum luminosity produced, and the innermost layer reached by the bottom of the surface convective zone during the second dredge-up.

All the models undergo an off-center carbon ignition; the point at which the nuclear energy release is highest is more internal the higher is the mass, ranging from  $\sim 0.6M_{\odot}$  for  $M=6.5M_{\odot}$ , down to  $\sim 0.2M_{\odot}$  for  $M=8M_{\odot}$ . This early

**Table 1.** Carbon burning properties

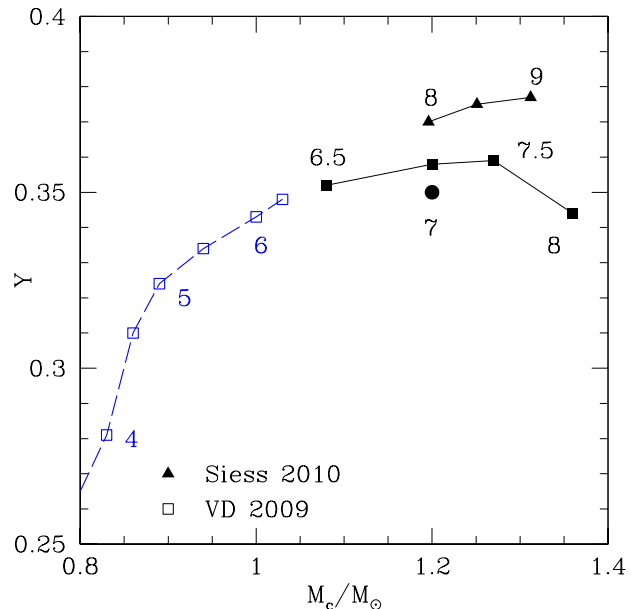
$M/M_{\odot}$	$\tau_{CB-HeB}(10^5)\text{yr}$	$M_{CO}$	$m_{ign}$	$L_C$	$M_{SDU}$
6.5	2.3	1.06	0.60	7.1(6)	1.15
7.0	2.0	1.12	0.50	2.3(6)	1.20
7.5	1.7	1.18	0.36	1.0(6)	1.30
8.0	1.4	1.29	0.21	6.3(5)	1.40

**Figure 1.** Kippenhahn diagram showing the temporal behaviour of the development of convective regions during the C-burning phase of a  $7M_{\odot}$  model.

phase of carbon burning is followed by the development of a convective flame, that proceeds inwards. In all the models investigated, this instability region eventually reaches the center, and forms a O-Ne core, with the only exception of the  $6.5M_{\odot}$  model, that is left with a core made up of carbon and oxygen; in this latter model carbon burning is aborted, in analogy to the behaviour of the masses just above the limit for carbon ignition, described by Doherty et al. (2010). The formation of the O-Ne core is followed by other off-center carbon burning episodes, whose intensity becomes progressively lower, after which the TPs phase begins. Fig. 1 shows a Kippenhahn diagram for the model with mass  $7M_{\odot}$ , indicating the borders of the convective shells that form as a consequence of carbon ignition, and the base of the external convective mantle. A detailed analysis of the C-burning phase is beyond the scopes of the present work: the interested reader may find in Siess (2006) a detailed physical description of the C-burning phase in super-AGB stars.

### 3.3 How much helium is produced by SAGBs?

The second dredge-up is a common feature of all the models investigated; the evolutionary stage at which it takes place depends on the initial mass: it is prior to C-burning in all the models, apart from the  $8M_{\odot}$  case, in which it occurs after the formation of the ONe core. This behaviour is in agreement

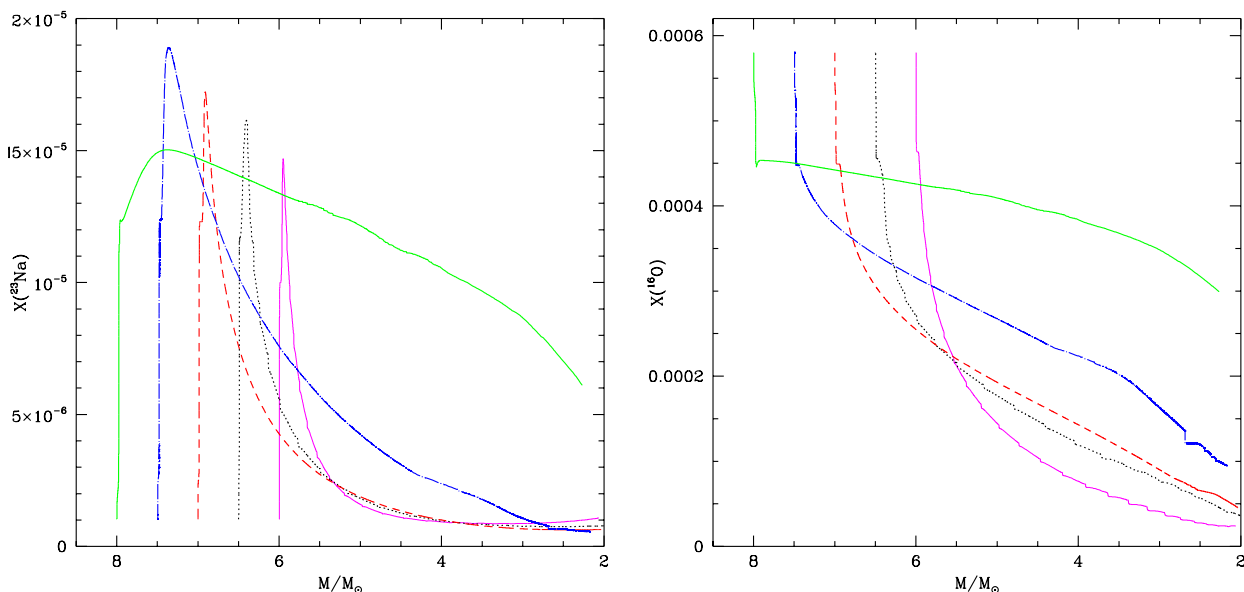
**Figure 2.** The helium content of the ejecta of the massive AGB (open squares, from Ventura & D’Antona 2009) and of the SAGB models calculated in this work (full squares) is shown as a function of the core mass. The numbers next to the points indicate the initial mass of the model. The values for the SAGBs by Siess (2010) (full triangles) for similar chemistry are shown. The full dot indicates how the helium content from the  $7M_{\odot}$  decreases when a shallower mass loss formulation is adopted.

with the investigation by Garcia-Berro et al. (1997). On the chemical side, the main consequence of the second dredge-up is the increase in the helium mass fraction, up to  $Y \simeq 0.36$  (see column 4 in Table 2). This is the maximum enrichment of helium that is produced by SAGBs according to the present investigation. It is in reasonable agreement, though a bit lower, than the helium yields by Siess (2010) for the same metallicity. Figure 2 shows the abundances in the ejecta of the massive AGBs from Ventura & D’Antona (2009) (open squares) and of the present models (full squares), as a function of the core mass (CO cores from 4 to  $6.5M_{\odot}$ , ONe cores for larger mass).

Our SAGB models do not provide helium abundances as large as  $Y \sim 0.40$  invoked to interpret the bMS in  $\omega$  Cen (Sollima et al. 2007) and NGC 2808 (Piotto et al. 2007). Notice however that the values depend on the interpretation of the MS colors, on which uncertainties may be large (Portinari et al. 2010).

**Table 2.** Properties of SAGB models and average abundances in the ejecta

$M/M_{\odot}$	$M_c/M_{\odot}$	$T_{\text{bce}}^{\text{max}}/10^8$	Y	$^{16}\text{O}/\text{Fe}$	$[\text{Na}/\text{Fe}]$	$[\text{Mg}/\text{Fe}]$	$^{27}\text{Al}/\text{Fe}$	A(Li)	$\dot{M}$ law	$M_{\text{tot}}^f/M_{\odot}$	$M_c^f/M_{\odot}$	NTP
6.5	1.08	1.16	0.352	-0.24	0.32	0.226	0.80	2.36	B95	1.70	1.10	32
7.0	1.20	1.20	0.358	-0.15	0.39	0.253	0.74	2.12	B95	1.99	1.23	38
7.5	1.27	1.27	0.359	0.01	0.67	0.289	0.57	2.75	B95	2.15	1.29	48
8.0	1.36	1.47	0.344	0.20	1.00	0.290	0.40	4.39	B95	2.20	1.38	53
7.0	1.20	1.34	0.350	-0.69	0.17	0.09	0.54	2.58	VW93	2.15	1.24	348


**Figure 3.** Left panel: The variation during the evolution of the sodium abundance at the surface of models with initial masses  $6M_{\odot}$  (light solid line),  $6.5M_{\odot}$  (dotted),  $7M_{\odot}$  (dashed),  $7.5M_{\odot}$  (dot-dashed),  $8M_{\odot}$  (solid); Right panel: the same as the left panel, but for the oxygen surface mass fraction.

### 3.4 The effects of HBB

Tab. 2 shows the main properties of the TP phase of our models, i.e. the core mass at the first thermal pulse, the maximum temperature reached at the base of the convective mantle, the average chemistry of the ejecta, the mass of the core and of the whole star when the computations stopped, and the number of thermal pulses experienced.

During the TP phase no extra-mixing was considered from any convective border, and no appreciable third dredge-up was experienced by any of our models: the surface chemistry changes only for the effects of HBB.

Fig. 3 shows the behaviour of the surface oxygen (right) and sodium (left), as the envelope mass is consumed. To show the continuity with the previous investigations, limited to models not undergoing any carbon burning, we also show the evolution of a  $6M_{\odot}$  model, taken from Ventura & D’Antona (2008). Oxygen is destroyed in all models during the thermal pulses phase. Despite the higher temperatures attained at the bottom of the convective envelope in the more massive models (see Table 2), the higher mass loss experienced (due to the larger luminosity) favours a flatter oxygen vs. mass relationship, because a lot of mass is lost before the oxygen is burnt in great quantities.

The average oxygen content of the ejecta, which in Ta-

ble 2 is expressed in terms of  $[\text{O}/\text{Fe}]^2$  is found to increase with mass; this trend agrees with the previous findings by Ventura & D’Antona (2009) (most massive AGBs) and by Siess (2010) (SAGBs), and indicates that the stars whose ejecta show the most extreme chemistries are those close to the limit for carbon ignition.

The behaviour of sodium is more tricky. The maximum sodium produced increases with mass (as a consequence of the larger temperatures attained at the bottom of the convective envelope), with the only exception of the  $8M_{\odot}$  model, that achieves the second dredge-up after the C-burning phase, and evolves rapidly to high temperatures: in this case sodium begins to be destroyed before the early increase, normally associated to the conversion of the  $^{22}\text{Ne}$  transported to the surface by the second dredge-up. Similarly to oxygen, the sodium content of the ejecta increases with mass (see Table 2).

The simultaneous behaviour of oxygen and sodium abundance at the surface of these stars along their evolution is shown in Fig.4. We used the quantity  $[X/\text{Fe}]$  on both axes. We see that all the models follow the same qualitative

<sup>2</sup> Here we use the standard notation, by indicating with  $[X/\text{Fe}]$  the quantity  $\log(X/\text{Fe}) - \log(X/\text{Fe})_{\odot}$ .

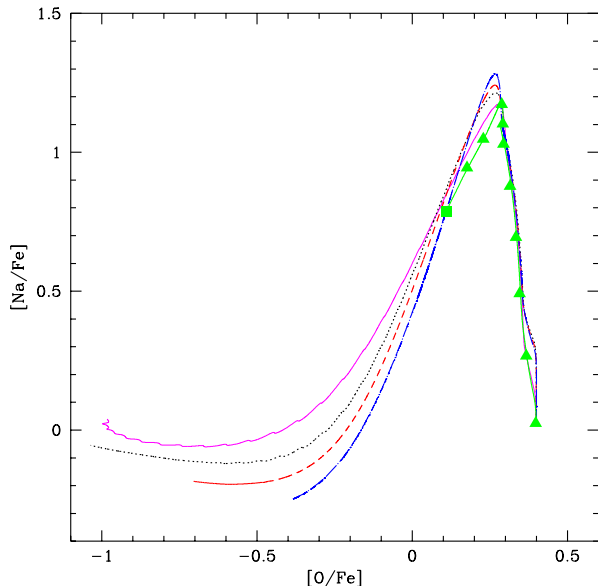


**Figure 4.** The simultaneous variation of the surface abundances of oxygen and sodium in the SAGB models presented in this investigation. The labels are the same as in the two panels of Fig.3. For clarity reasons, the path followed by the  $8M_{\odot}$  model is indicated by solid triangles, and is terminated by the full square

behaviour, with an initial anticorrelated phase, during which oxygen is reduced whereas sodium increases, and a following phase, when both elements are destroyed at the bottom of the external envelope.

Oxygen is destroyed with continuity until the envelope is removed completely, whereas sodium follows an approximately asymptotic behaviour, that corresponds to the aforementioned balance between the production and the destruction channels. The curves corresponding to the more massive models (see in particular the evolution of the  $8M_{\odot}$  model, indicated by solid triangles and by the full square pointing the end of the evolution), stop at a stage when the oxygen and sodium abundances are still large, because the strong mass loss favoured a rapid consumption of the whole envelope, before the surface mass fractions of both elements could diminish to nominal values.

The variation of the surface contents of magnesium and  $^{27}\text{Al}$  is shown in Fig.5. We note that a stronger production of aluminium is achieved in the models of smaller mass, because in the most massive stars the strong mass loss prevents an advanced Mg-Al nucleosynthesis, and only a modest increase in the surface aluminium is reached.

#### 4 HOW SENSITIVE ARE THE YIELDS TO THE DETAILS OF SAGB MODELLING?

Before turning to the impact of these results on the interpretation of the chemical anomalies observed in GC stars, and on the self-enrichment scenario by massive AGBs, we try to understand how robust these results are, and their sensitivity to the various uncertainties (convection, mass loss, cross-sections) affecting the SAGB modelling.

The recent exploration by Doherty et al. (2010) re-

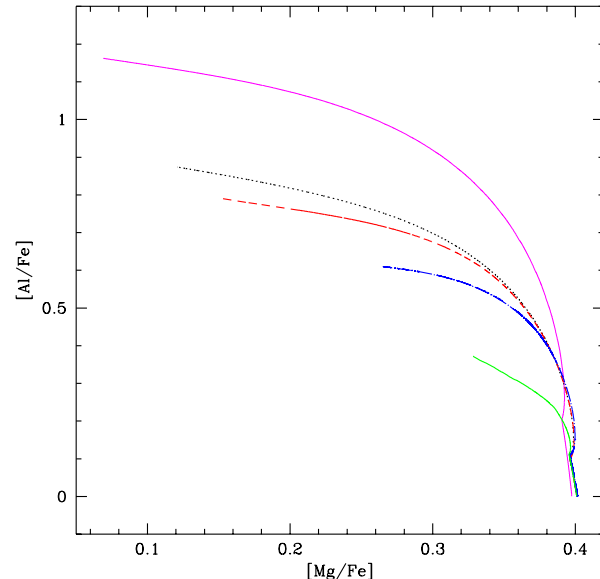


**Figure 5.** The simultaneous variation of the surface abundances of magnesium and aluminium in the SAGB models presented in this investigation. The labels are the same as in the two panels of Fig.3.

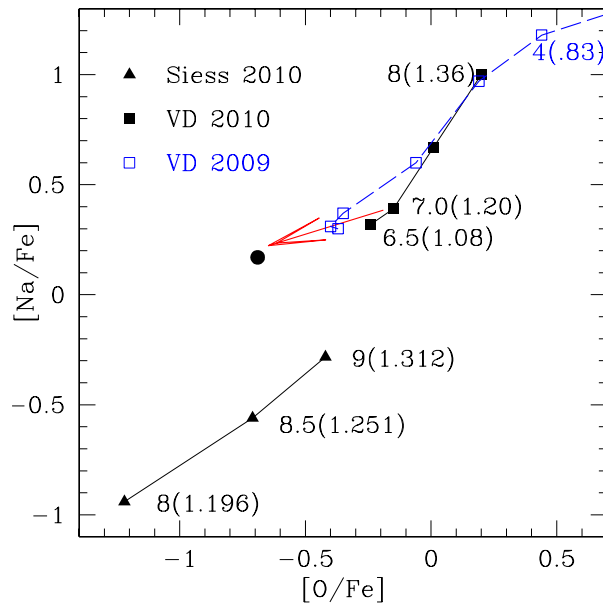


**Figure 6.** The average  $[\text{O}/\text{Fe}]$  and  $[\text{Na}/\text{Fe}]$  content of the ejecta of the SAGB models by Siess (2010) (full triangles), and those calculated in this work (full squares). Open squares denote the massive AGB yields by Ventura & D'Antona (2009). The numbers next to the points indicate the initial mass of the model, and the core mass (in parenthesis). The arrow indicates how the yields of the  $7M_{\odot}$  model change when the lower mass loss formulation is adopted (see Table 1).

vealed a great homogeneity among the results obtained with different codes, that confirm the results concerning the C-burning phase already present in the literature. These models are limited to the evolutionary phases preceding the first thermal pulse, whereas as far as we know the only full investigation extended to the whole SAGB evolution was given by Siess (2010).

Fig. 6 shows a comparison between the yields of SAGB models by Siess (2010) (indicated as full triangles) and those found in the present investigation (open squares), in the  $[\text{Na}/\text{Fe}]$  vs  $[\text{O}/\text{Fe}]$  plane. In both cases the points move towards the top-right of the plane with increasing mass. The yields by Siess (2010) show lower contents of oxygen and sodium. The differences in  $[\text{O}/\text{Fe}]$  are mostly due to the different modelling of mass loss. The treatment by Vassiliadis & Wood (1993), used by Siess (2010), favours much smaller rates, thus leading to a very advanced nucleosynthesis at the bottom of the outer convective zone. Conversely, the recipe by Bloeker (1995) determines much higher  $\dot{M}$ s, so that the mass of the envelope is lost before a great destruction of oxygen can be achieved. This is confirmed by the full dot in Fig.6, that indicates the yield found in the  $7M_{\odot}$  model when the Vassiliadis & Wood (1993) rate is adopted: the theoretical point is shifted in the range of oxygen abundances predicted by Siess (2010). The remaining difference is due to the fact that our initial mixture is alpha-enhanced with  $[\alpha/\text{Fe}] = +0.4$ , whereas the mixture used by Siess (2010) is solar-scaled. The sodium yields remain different, our  $[\text{Na}/\text{Fe}]$  being systematically larger. This can be attributed to the different nuclear reaction rates adopted, in particular for what concerns the proton capture reaction by  $^{22}\text{Ne}$  nuclei, for which we adopted the highest rates from the Hale et al. (2002) compilations, whereas the recommended rate was used by Siess (2010).

The comparison for what concerns the magnesium and aluminium content is more tricky, because of the differences in the assumptions made, that involve the nuclear cross-sections, the initial magnesium abundances, and the mass loss description. The Al yields by Siess (2010) decrease with mass, starting from  $[\text{Al}/\text{Fe}] = 0.27$  for the  $M = 8M_{\odot}$  model, down to  $[\text{Al}/\text{Fe}] = 0.18$  for  $M = 9M_{\odot}$ . Our yields show the same trend (see col.8 in Table 2), but the values are systematically higher, mainly because our alpha-enhanced mixture has a higher initial content of magnesium.

This investigation indicates that the oxygen and sodium yields in SAGBs vary considerably according to the treatment of mass loss: when a modest mass loss is adopted, extreme chemistries are possible, because a very advanced nucleosynthesis can be achieved at the bottom of the convective envelope. Convective modelling is also expected to play a role in determining the yields of SAGBs (see the discussion in Siess (2010)), although the effects are less important than for AGBs, because a more efficient convective modelling would determine higher temperatures, but also a larger mass loss, and the two effects tend to compensate for what concerns the stage of nucleosynthesis achieved.

In the near future, it could be possible to calibrate the mass loss rate by achieving constraints from the abundances of stars belonging to the bMS in the clusters  $\omega$  Cen and NGC 2808, in the hypothesis that the bMS stars are directly formed from the ashes of SAGBs (Pumo et al. 2008; D’Ercole et al. 2008).

## 5 CONCLUSIONS

We present the evolution of the main physical and chemical properties of stars with initial mass in the range  $6.5\text{--}8M_{\odot}$ , which, according to our choice for the overshooting from the convective core during the H- and He-burning phases, undergo carbon ignition in conditions of partial degeneracy. Our findings concerning the modalities of carbon burning, the inwards propagation of the convective flame that is developed, and the final chemistry of the O-Ne core, are in agreement with the results presented by other research groups.

The same homogeneity cannot be expected for the following TP phase, because its physical and chemical evolution is determined by the treatment of two still poorly known physical processes: mass loss and turbulent convection. We focused our analysis on the chemistry of the ejecta of SAGBs, and in particular on the oxygen, sodium and aluminium content, that have been shown to vary among stars in globular clusters.

The models presented here attain extremely large temperatures at the bottom of the convective envelope, which, in turn, favour an advanced nucleosynthesis, i.e. very small abundances of oxygen and sodium, and a strong production of aluminium. These findings, which are in fairly good agreement with the results obtained by Siess (2010), hold in case that mass loss is modelled according to Vassiliadis & Wood (1993). Conversely, when the Bloeker (1995) recipe is used, the nucleosynthesis at the bottom of the external mantle is halted by the general cooling of the structure favoured by the fast consumption of the envelope, so that a less extreme chemistry is achieved. In this latter case higher abundances of oxygen and sodium are produced, and, in the overall context of a possible pollution in GCs produced by massive AGBs and super-AGBs, gas with the most extreme chemistry is expected to be ejected by masses around  $6M_{\odot}$ .

Helium is produced in great quantities in all cases, with a maximum of  $Y \sim 0.36$  for the highest masses. In the framework of our models, abundances larger than this value for the extreme populations in the most massive clusters cannot be explained by formation from SAGB ashes. However, the values derived from observations are still largely uncertain (Portinari et al. 2010).

If the bMS stars in massive GCs are formed directly from the ejecta of SAGBs, future spectroscopic analysis will help understanding the reliability of the self-enrichment scenario by massive AGBs, and, eventually, will help to calibrate the poorly constrained mass loss in the SAGB phase. In the end, this calibration may also be important to constrain the mass range in which we expect that the core grows up to begin electron capture on the Ne nuclei. Indirect informations on the formation of neutron stars by the e-capture supernova channel in single stars will be eventually achieved (Poelarendes et al. 2008).

## ACKNOWLEDGMENTS

The authors are indebted to the referee, Lionel Siess, for the many detailed comments and suggestions, that helped improving the quality of the manuscript.

## REFERENCES

- Angulo C., Arnould M., Rayet M., et al., 1999, Nucl.Phys. A, 656, 3
- Bedin, L. R., Piotto, G., Anderson, J., Cassisi, S., King, I. R., Momany, Y., Carraro, G. 2004, ApJ, 605, L125
- Blöcker T., 1995, A&A, 297, 727
- Blöcker T., Schönberner D., 1991, A&A, 244, L43
- Caloi, V., & D'Antona, F. 2007, A&A, 463, 949
- Canuto V.M.C., Mazzitelli I., 1991, ApJ, 370, 295
- Carretta E., 2006, AJ, 131, 1766
- Carretta E., Bragaglia A., Gratton R.G., Lucatello S., Catanzaro G., et al., 2009a, A&A, 505, 117
- Carretta E., Bragaglia A., Gratton R.G., Lucatello S., 2009b, A&A, 505, 139
- Cloutman L.D., Eoll J.G. 1976, ApJ, 206, 548
- Cohen J.G., Melendez J. 2005, AJ, 129, 303
- Cottrell P.L., Da Costa G.S. 1983, ApJ, 245, L79
- D'Antona, F., Bellazzini, M., Caloi, V., Pecci, F. F., Galletti, S., & Rood, R. T. 2005, ApJ, 631, 868
- D'Ercole A., Vesperini E., D'Antona, F., Mc Millan S.L.W., Recchi, S., 2008, MNRAS, 391, 825
- D'Ercole A., D'Antona, F., Ventura, P., Vesperini E., Mc Millan S.L.W., 2010, MNRAS, 407, 854
- Decressin T., Meynet G., Charbonnel C., Prantzos N., Ekström S., 2007, A&A, 464, 1029
- Denissenkov, P.A., Herwig, F., 2003, ApJ, 590, L99
- de Mink, S.E., Pols, O.R., Langer, N., Izzard, R.G., 2009, A&A, 507, L1
- Doherty C. L., Siess L., Lattanzio J. L., Gil-Pons P., 2010, MNRAS, 401, 1453
- Formicola A., Imbriani G., Costantini H., 2004, Phys. Lett. B, 591, 61
- Garcia-Berro E., Iben I.J., 1994, ApJ, 434, 306
- Garcia-Berro E., Ritossa C., Iben I.J., 1997, ApJ, 485, 765
- Gil-Pons P., Gutierrez J., Garcia-Berro E., 2007, A&A, 464, 667
- Grevesse N., Sauval A.J, 1998, SSRv, 85, 161
- Hale S.E., Champagne A.E., Iliadis C., et al., 2002, Phys.Rev. C, 65, 5801
- Hale S.E., Champagne A.E., Iliadis C., et al., 2004, Phys.Rev. C, 70, 5802
- Herwig, F. 2004, ApJS, 155, 651
- Iben I.J., Ritossa C., Garcia-Berro E., 1997, ApJ, 489, 772
- Izzard R.G., Lugaro M., Karakas A.I., Iliadis C., van Raai M., 2007, A&A, 466, 641
- Karakas, A., & Lattanzio, J. C. 2007, Publications of the Astronomical Society of Australia, 24, 103
- Norris J., Cottrell P.L., Freeman K.C., Da Costa G.S., 1981, ApJ, 244, 205
- Norris, J. E. 2004, ApJ Letters, 612, L25
- Paczynski B., 1970, Acta Astron., 20, 47
- Piotto, G., et al. 2005, ApJ, 621, 777
- Piotto, G., et al. 2007, ApJ Letters, 661, L53
- Poelarendes A.J.T., Herwig F., Langer N., Heger A., 2008, ApJ, 675, 614
- Portinari, L., Casagrande, L., & Flynn, C. 2010, MNRAS, 801
- Pumo, M. L., D'Antona, F., & Ventura, P. 2008, ApJ, 672, L25
- Ritossa C., Garcia-Berro E., Iben I.J., 1996, ApJ, 460, 489
- Ritossa C., Garcia-Berro E., Iben I.J., 1999, ApJ, 630, L73
- Siess, L., 2006, A&A, 448, 717
- Siess, L., 2007, A&A, 476, 893
- Siess, L., 2009, A&A, 497, 463
- Siess, L., 2010, A&A, 512, A10
- Sills A., Glebbeek E., 2010, MNRAS, 407, 277
- Sollima A., Ferraro F. R., Bellazzini M., Origlia L., Straniero O., Pancino E., 2007, ApJ, 654, 915
- Vassiliadis E., Wood P.R., 1993, A&A, 413, 641
- Ventura P., D'Antona F., 2005a, A&A, 341, 279
- Ventura P., D'Antona F., 2005b, A&A, 439, 1075
- Ventura P., D'Antona F., 2008, A&A, 479, 805
- Ventura P., D'Antona F., 2009, A&A, 499, 835
- Ventura P., D'Antona F., Mazzitelli I., Gratton, R., 2001, ApJ, 550, L65
- Ventura P., Zeppieri A., Mazzitelli I., D'Antona F., 1998, A&A, 334, 953